Cell Stem Cell
Resource

Gene Targeting of a Disease-Related Gene in Human Induced Pluripotent Stem and Embryonic Stem Cells

Jizhong Zou,[1] Morgan L. Maeder,[6] Prashant Mali,[1,2] Shondra M. Pruett-Miller,[7] Stacey Thibodeau-Beganny,[6] Bin-Kuan Chou,[1,3] Guibin Chen,[1] Zhaohui Ye,[1,4] In-Hyun Park,[8,9,11] George Q. Daley,[8,9,11] Matthew H. Porteus,[7,*] J. Keith Joung,[6,10,*] and Linzhao Cheng[1,3,4,5,*]
[1]Stem Cell Program, Institute for Cell Engineering
[2]Graduate Program in Biomedical Engineering
[3]Graduate Program in Cellular and Molecular Medicine
[4]Graduate Program in Immunology
[5]Department of Gynecology and Obstetrics
Johns Hopkins University School of Medicine, Baltimore, MD 21205, USA
[6]Molecular Pathology Unit, Center for Cancer Research, and Center for Computational and Integrative Biology, Massachusetts General Hospital, Charlestown, MA 02129, USA
[7]Departments of Pediatrics and Biochemistry, University of Texas Southwestern Medical Center, Dallas, TX 75390, USA
[8]Division of Pediatric Hematology/Oncology, Children's Hospital Boston, Boston, MA 02115, USA
[9]Department of Biological Chemistry and Molecular Pharmacology
[10]Department of Pathology
Harvard Medical School, Boston, MA 02115, USA
[11]Harvard Stem Cell Institute, 42 Church Street, Cambridge, MA 02138, USA
*Correspondence: matthew.porteus@utsouthwestern.edu (M.H.P.), jjoung@partners.org (J.K.J.), lcheng@welch.jhu.edu (L.C.)
DOI 10.1016/j.stem.2009.05.023

SUMMARY

We report here homologous recombination (HR)-mediated gene targeting of two different genes in human iPS cells (hiPSCs) and human ES cells (hESCs). HR-mediated correction of a chromosomally integrated mutant GFP reporter gene reaches efficiencies of 0.14%–0.24% in both cell types transfected by donor DNA with plasmids expressing zinc finger nucleases (ZFNs). Engineered ZFNs that induce a sequence-specific double-strand break in the GFP gene enhanced HR-mediated correction by > 1400-fold without detectable alterations in stem cell karyotypes or pluripotency. Efficient HR-mediated insertional mutagenesis was also achieved at the endogenous *PIG-A* locus, with a > 200-fold enhancement by ZFNs targeted to that gene. Clonal *PIG-A* null hESCs and iPSCs with normal karyotypes were readily obtained. The phenotypic and biological defects were rescued by *PIG-A* transgene expression. Our study provides the first demonstration of HR-mediated gene targeting in hiPSCs and shows the power of ZFNs for inducing specific genetic modifications in hiPSCs, as well as hESCs.

INTRODUCTION

Human embryonic stem cells (hESCs) derived from blastocyst-stage embryos can self-renew indefinitely in culture while retaining their pluripotency (Reubinoff et al., 2000; Thomson et al., 1998). Recently, human somatic cells have been successfully reprogrammed into induced pluripotent stem cells (iPSCs) that exhibit unique characteristics similar to hESCs (Lowry et al., 2008; Mali et al., 2008; Park et al., 2008; Takahashi et al., 2007; Yu et al., 2007). Patient-specific iPSCs hold enormous promise for personalized cell replacement therapy, as well as for research of various human diseases. Full utilization of these human pluripotent stem cells (hPSCs) will require the development of efficient methods for performing gene targeting, a sequence-specific and permanent genome modification that exploits the cell's ability to perform homologous recombination (HR). Gene targeting by HR has played a critical role in genetic studies of various systems, including the generation of knockout/knockin transgenic mouse models using mouse ESCs. The efficiency of HR-mediated gene targeting in hESCs, however, remains low even 10 years after its first report (Thomson et al., 1998), with only few successful studies published to date using the method that is routinely performed in mouse ESCs (Costa et al., 2007; Davis et al., 2008; Di Domenico et al., 2008; Irion et al., 2007; Ruby and Zheng, 2009; Urbach et al., 2004; Zwaka and Thomson, 2003). Using standard plasmid-based systems, the current HR rate is $< 10^{-6}$ in karyotypically normal hESCs and other nontransformed mammalian cells. Moreover, to date, there has been no report on successful gene targeting in hiPSCs. One reason that gene targeting in hPSCs is more difficult is because they grow poorly as single cells (a practice required for selection of rare targeted clones), compared with mouse ESCs. Thus, strategies that increase the efficiency of gene targeting in hPSCs would improve both the therapeutic and experimental potential of these cells.

Zinc finger nucleases (ZFNs) are engineered sequence-specific nucleases consisting of a customized array of zinc

fingers engineered to bind to a specific DNA sequence and a nonspecific DNA endonuclease domain (Durai et al., 2005; Porteus and Carroll, 2005). Each zinc finger domain recognizes 3–4 bp of DNA, and a three-finger ZFN recognizes a 9–10 bp DNA sequence. When two ZFNs bind their cognate target sequence in the proper orientation, the nuclease domain is able to dimerize and create a sequence-specific double-stranded break (DSB). The ZFN-induced DSB can then be repaired with high efficiency by either HR or error-prone nonhomologous end-joining (NHEJ), independent of a DNA template for repair. Therefore, ZFNs induce a site-specific insertion or deletion at the site of the break after NHEJ or a defined genetic modification near the site of the DSB by HR with an exogenous donor DNA fragment. ZFNs have been used to make site-specific genomic modifications with high efficiencies in a variety of cell lines and several small organisms (Carroll, 2008). A recent study showed that ZFNs can enhance gene targeting in human ES cells using integrase-defective lentiviral vectors (IDLVs) to deliver both ZFN expression cassettes and an HR donor DNA template (Lombardo et al., 2007). Limitations of this study, such as lack of data by Southern blotting for confirming the HR event and excluding random integration of the donor DNA, have been noted by the authors of a recent review (Giudice and Trounson, 2008). Another limitation of this work is that the two hESC lines used are prone to karyotypic abnormalities after prolonged culture (Cowan et al., 2004). Such abnormalities likely contribute to their favorable growth characteristics in culture and can affect gene-targeting efficiencies. Whether ZFNs might induce chromosomal alterations and changes in growth parameters of targeted hESCs has not been reported. Although the use of IDLVs reduces the rate of vector integration substantially, it does not eliminate such integration events (Mali et al., 2008; Nightingale et al., 2006).

In this study, we used a virus-free system to perform ZFN-enhanced gene targeting at the endogenous *PIG-A* gene and at a defective, chromosomally integrated enhanced green fluorescent protein (EGFP) reporter gene in both hESCs and human iPSCs (hiPSCs). The *PIG-A* gene is required for the retention of dozens of glycosyl-phosphatidyl-inositol-anchored proteins (GPI-APs) on the cell surface and is mutated in hematopoietic stem cells from patients with the blood disorder paroxysmal nocturnal hemoglobinuria (PNH). The defective, chromosomally integrated EGFP reporter gene that we used in our studies requires HR to reconstitute a full-length gene and thereby restore fluorescence. We demonstrate that the transient expression of sequence-specific ZFNs significantly enhanced HR (2400-fold increase) in hESCs and that we were able to readily obtain *PIG-A* null hESCs by both HR and mutagenic NHEJ. Importantly, we also show that these ZFNs enhance gene targeting without detrimental effects on either cell karyotypes or pluripotency. Moreover, we also provide the first demonstration that ZFNs can enhance gene targeting in two hiPSC lines by successfully performing targeted HR events at both the *PIG-A* locus and a chromosomally integrated EGFP reporter gene. The present study describes and validates publicly available ''open-source'' reagents and protocols that will enable researchers to use ZFNs to efficiently create or correct specific mutations at their genes of interest in hiPSCs and hESCs.

RESULTS

Using an EGFP Gene Reporter System to Optimize Gene Targeting in hESCs

To enhance the efficiency of gene targeting in hESCs by nonviral vectors, we developed better methods for plasmid delivery and for selection of rare transgenic hES clones. First, we established an immortalized feeder cell line (W3R) that expresses Wnt3a to promote hESC growth and coexpresses three drug-resistant genes (Cai et al., 2007). The ability of W3R feeder cells that support hESCs and are resistant to neomycin, hygromycin B, and puromycin allowed us to efficiently select rare clones of transfected hESCs expressing one of three drug-resistant genes: Neo^R, $Hygro^R$, or $Puro^R$. Second, we optimized methods for delivering plasmid DNA into hESCs using the Amaxa's improved electroporation method called nucleofection (Cai et al., 2007). Using this strategy, hESCs can be transfected with > 50% efficiency, and stable ESCs can be generated at a rate of 10^{-5} (Cai et al., 2007; Hohenstein et al., 2008). In this study, we used these optimized methods for plasmid delivery and selection to further improve gene targeting in hESCs.

To assess the efficiency of HR-mediated gene targeting in hESCs, we established a mutated GFP gene-based reporter system, similar to one previously described and used in somatic human cells (Porteus, 2006; Porteus and Baltimore, 2003). In this improved version, the EGFP gene was used to achieve a brighter GFP signal as compared to the GFPmut1 gene (Yang et al., 1996) used in the previous studies. A 35 bp DNA fragment containing a stop codon was inserted into the EGFP sequence, 12 bp downstream of a site for which we had previously generated ZFN pairs (Pruett-Miller et al., 2008). This mutated EGFP* cassette was inserted into a lentiviral vector that we designated EGIP* (Figure 1A). This EGIP* vector enables the creation of a chromosomally integrated EGFP* target sequence by lentiviral transduction in a variety of cell types, including hESCs. We also constructed a donor template plasmid called tGFP, which contains a truncated EGFP DNA. HR between the transfected tGFP donor and the integrated EGFP* target results in the reconstitution of a full-length EGFP gene without the insertion, and its gene expression restores GFP fluorescence. In 293T cells that can be transfected very efficiently by either lipofection or nucleofection, GFP+ correction rate was low (~7 per 10^6 cells) when cells were transfected by tGFP alone (Figure S1A available online). Cotransfection of the same reporter 293T cells with tGFP and two plasmids expressing ZFNs targeting a site in the EGFP gene (Pruett-Miller et al., 2008) led to an increase in the level of GFP+ cells to ~3% (Figures S1B and S1C): a > 4000-fold enhancement (Figure S1A). The percentage of GFP+ population remained stable over 2 weeks after transfection, indicating minimal cytotoxicity of ZFNs used in these experiments (Figure S1D).

We next used the EGFP* HR system in hESCs after stable integration of the EGIP* reporter vector. Using conditions that we had previously established for nucleofection of hESCs (Cai et al., 2007), we were able to achieve a transient transfection efficiency of 50%–70% for multiple hES lines, each bearing a stably integrated EGIP* reporter vector (data not shown). Following transfection of the tGFP donor DNA (Figure 1A), we measured EGFP gene correction in hESCs (harboring the EGFP* reporter)

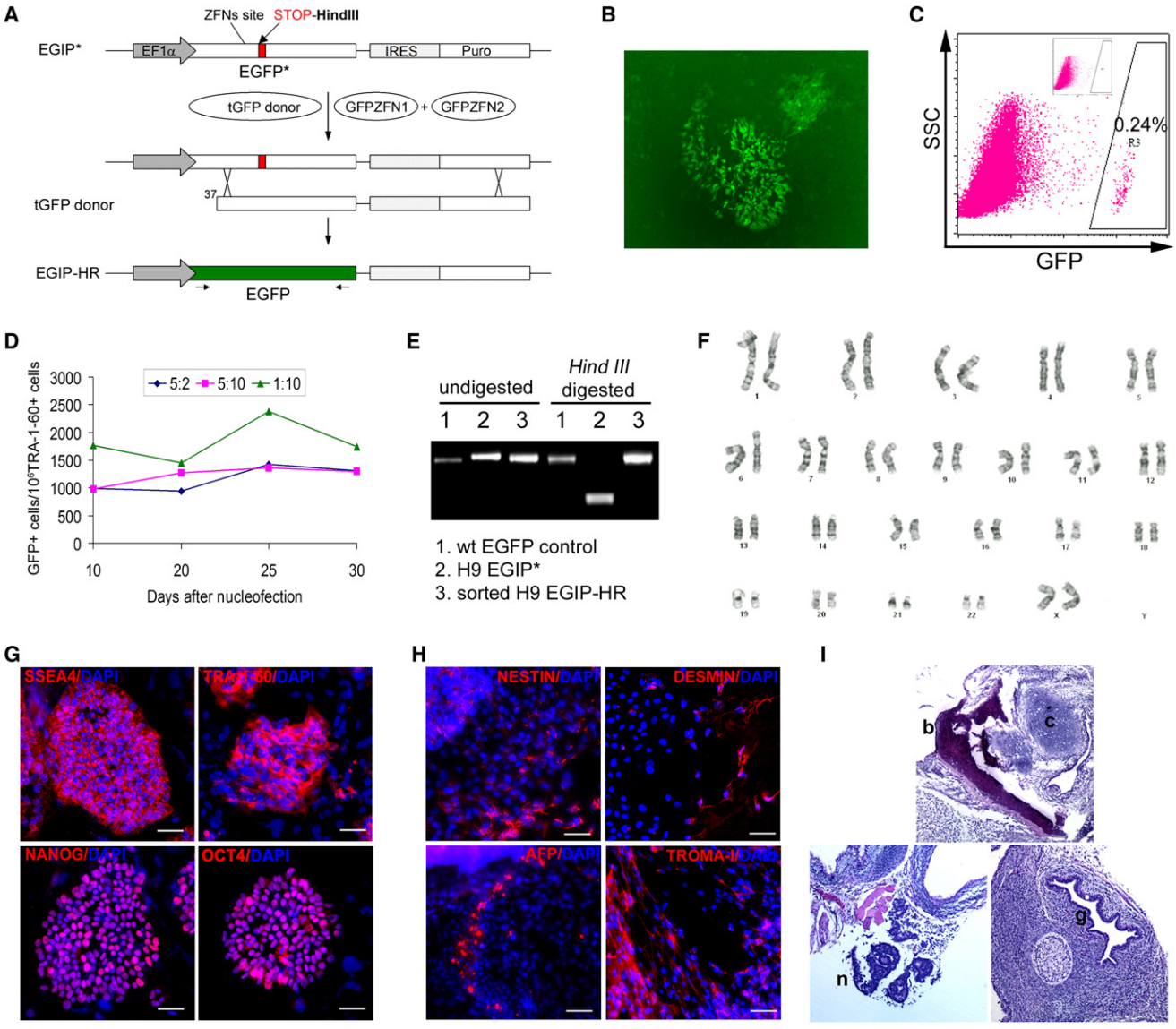

Figure 1. Correction of a Mutant EGFP Reporter Gene by ZFN-Mediated Gene Targeting

(A) Scheme of the EGFP gene correction strategy. An enhanced GFP gene was mutated (EGFP*) by the insertion of a 35 bp fragment containing a translational stop codon and a *Hind III* site positioned 12 bp downstream of the GFP ZFN target site. The defective EGFP(*) transgene was delivered and integrated into human cells by a lentiviral vector called EGIP*. For EGFP gene correction, a repair donor (tGFP) containing 5′ truncated EGFP coding sequence was cotransfected with two plasmids expressing a pair of GFP-targeting ZFNs (GFPZFN1 and GFPZFN2). If HR-mediated repair occurs, expression of the wild-type EGFP gene will be restored. Arrows below the corrected EGFP gene represent primers used to detect the restored full-length EGFP gene.

(B) Fluorescence microscopy of EGFP gene correction with ZFNs in H9-EGIP* hESCs at day 7 postnucleofection.

(C) FACS analysis showing that the efficiency of ZFN-mediated EGFP gene correction in H9-EGIP* is as high as 0.24% (gated on TRA-1-60+ hESCs). Inset shows that no GFP+ cells are detected in 10^6 cells collected in the absence of GFP-specific ZFNs.

(D) Numbers of corrected GFP+ cells (per million of TRA-1-60+ hESCs) were monitored by FACS for 30 days. Three different ratios of donor:ZFNs were used at 5:2, 5:10, and 1:10. A ratio (w/w) of 1:10 is equivalent to a molar ratio of 1 donor DNA for 6.1 molecules of each ZFN.

(E) PCR amplification of wild-type EGFP gene using primers indicated in (A). H9-EGIP* template contains a *Hind III* site; therefore, PCR product can be digested by *Hind III* (sample 2). After ZFN-mediated HR, GFP+ cells were sorted and showed restoration of the wild-type EGFP gene without the *Hind III* site (1 and 3).

(F) H9 EGIP cells after ZFN-mediated HR show a normal karyotype (46, XY).

(G) H9 EGIP cells after ZFN-mediated HR maintain expression of pluripotency markers such as SSEA4, TRA-1-60, NANOG, and OCT4 after expansion by long-term culture. Scale bar, 50 μm.

(H) Immunostaining of embryoid body (EB) formed by H9 EGIP cells after ZFN-mediated HR. Day 14 EB shows ectoderm (NESTIN), mesoderm (DESMIN), endoderm (AFP), and trophectoderm (TROMA-I) markers. Scale bar, 50 μm.

(I) Teratoma formation of H9 EGIP cells after ZFN-mediated HR. H&E staining indicates in vivo differentiation of ectodermal (n, neuroepithelial), mesodermal (b, bone; c, cartilage), and endodermal (g, glandular epithelial) structures.

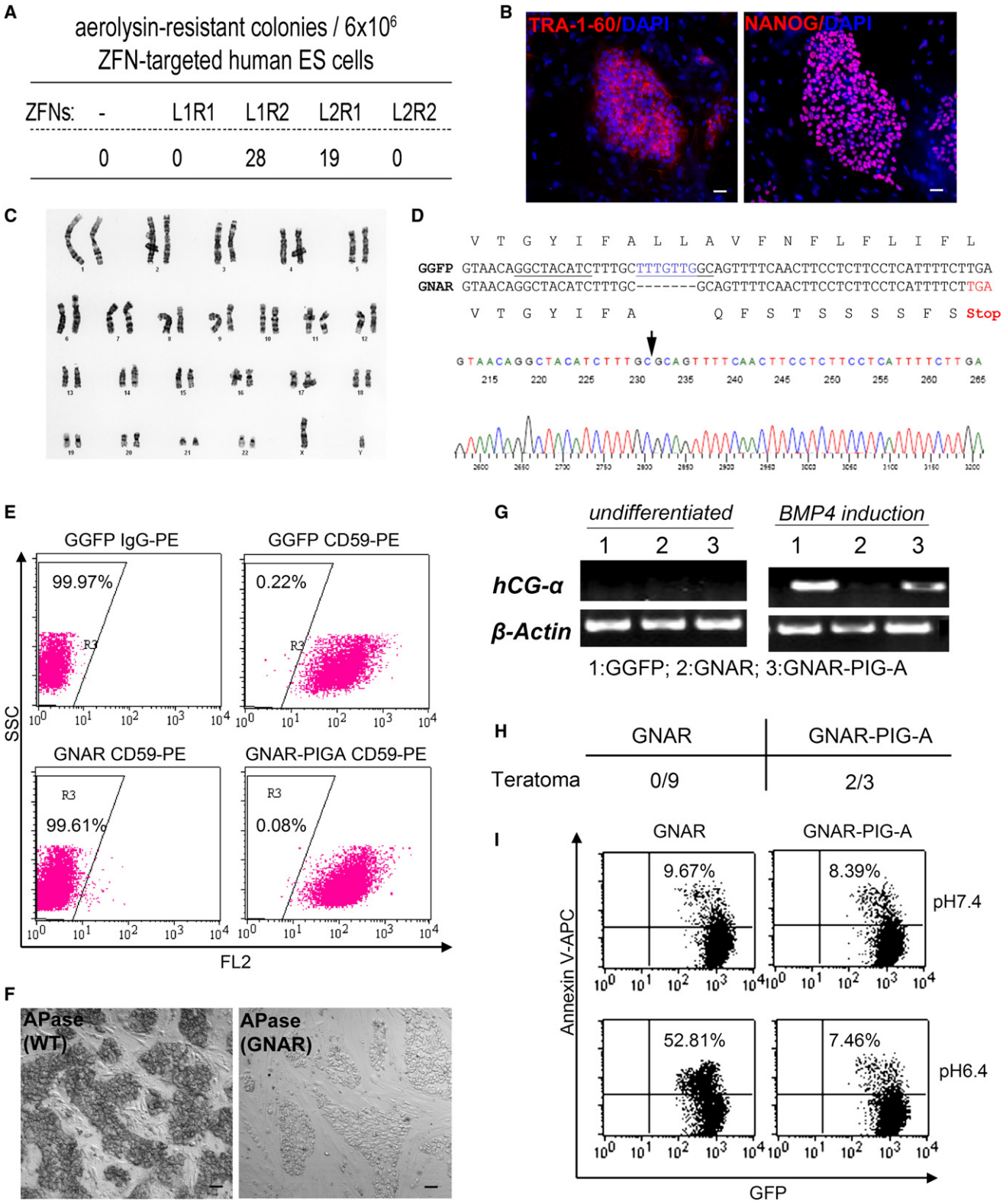

Figure 2. Generation of *PIG-A* Null Mutants by ZFN-Mediated NHEJ in H1 hESCs

(A) Four combinations of ZFN pairs targeting the *PIG-A* gene were tested for their abilities to induce mutagenic NHEJ in H1 (XY) hESCs that constitutively express GFP (GGFP). GGFP hESCs were first transfected by nucleofection with one of the four ZFN combinations (L1R1, L1R2, L2R1, L2R2) and expanded. At 17 days after nucleofection, expanded cells were treated with 0.5 nM aerolysin and allowed to form colonies for 7 days (Chen et al., 2008). The number of surviving colonies following aerolysin selection is shown.

with or without cotransfection of the GFP-ZFN expression plasmids. We observed that GFP+ cells in the hESC population at a frequency of up to 0.24% with ZFNs, compared to $< 10^{-6}$ without ZFNs, a > 2400-fold increase in the efficiency of HR in hESCs (Figures 1B and 1C). The level of GFP+ cells among the undifferentiated (TRA-1-60+) hESC population remained stable for at least 1 month following transfection of ZFN expression plasmids (Figure 1D). Correction of the EGFP* to the wild-type EGFP gene sequence was confirmed by both restriction digestion mapping and direct DNA sequencing (Figures 1E and S2).

Corrected GFP+ hESCs that had been obtained by ZFN-mediated HR retained normal karyotype, morphology, and expression of pluripotency markers even after long-term culture (>50 passages) (Figures 1F and 1G). Upon induction, they can also differentiate into three embryonic germ layers and trophoblast lineages via embryoid body (EB) formation in vitro (Figure 1H). When injected into immunodeficient mice, the corrected GFP+ cells formed teratomas containing cells representing all three embryonic germ layers (Figure 1I). These data indicate that our gene-targeting approach using transiently expressed ZFNs had no detectable adverse effects on the genome or pluripotency of hESCs.

Engineering and Validation of ZFNs Targeted to the Endogenous *PIG-A* Gene in hESCs

Because ZFNs can be engineered to recognize specific target DNA sequences, ZFN-enhanced gene targeting can potentially be used at any endogenous gene of interest. Therefore, we next wished to test whether ZFNs could enhance gene targeting of an actual endogenous human gene and focused our efforts on *PIG-A*, a gene that we had previously been unable to alter genetically using conventional gene-targeting methods. To create *PIG-A*-specific ZFNs, we used the oligomerized pool engineering (OPEN) platform recently developed (Maeder et al., 2008) and engineered four ZFN pairs for a site within the *PIG-A*-coding sequence. We chose to target such a sequence because we reasoned that mutation at that site would generate an inactive PIG-A protein.

We validated the four OPEN ZFN pairs targeting the *PIG-A* gene using a modified version of the EGFP* gene-targeting system described above, which contained the PIG-A ZFN target site inserted into the EGFP* gene, an approach similar to what has been used in previous studies (Porteus, 2006; Porteus and Baltimore, 2003; Urnov et al., 2005). We found that all four PIG-A ZFN pairs stimulated gene targeting by > 200-fold in 293T cells, with the L1/R2 pair showing the highest efficiency (Figure S3). We next tested these validated PIG-A ZFN pairs in hESCs by determining their ability to induce mutations in the endogenous *PIG-A* gene by mutagenic NHEJ repair of the ZFN-induced DSB. We used male (XY) hESCs such as H1 so that only one *PIG-A* gene (on the X chromosome) would need to be mutated to generate a phenotypic effect. Null mutants of *PIG-A* result in a loss of GPI-APs and, in turn, the resistance of targeted cells to aerolysin-mediated cell killing (Chen et al., 2008). It is important to note that *PIG-A* and GPI-APs have been shown to be dispensable for the growth of undifferentiated hESCs in culture (Chen et al., 2008). We utilized the aerolysin selection method to enumerate rare *PIG-A* null mutations and compared the activities of four PIG-A ZFN pairs in human H1-derived GGFP ESCs. The best pair of ZFNs (L1/R2) identified in the 293T EGFP* reporter assay also generated the greatest number of *PIG-A* mutant clones, creating 28 aerolysin-resistant colonies per 6×10^6 cells selected (Figure 2A).

One aerolysin-resistant hESC clone (called "GNAR") was chosen for further characterization. GNAR grew similarly to the parental cells from which it was derived, retained a normal karyotype, and displayed morphology and markers unique to hESCs (Figures 2B and 2C). DNA sequencing of the targeted region revealed deletion of 7 bp overlapping with the ZFN target sites, resulting in a frameshift mutation and a premature stop codon (Figure 2D). The *PIG-A* mutation in GNAR cells abolished the cell-surface expression of GPI-APs, such as CD59 (Figure 2E) and alkaline phosphatase (APase) (Figure 2F), as expected. The loss of GPI-APs in GNAR cells could be rescued by introduction of a *PIG-A* transgene, confirming that the defect in these cells is solely due to the lack of *PIG-A* expression (Figure 2E). Similarly, the loss of biological functions by GNAR hESCs can be restored by the *PIG-A* transgene expression in three different functional assays in vitro and in vivo (Figures 2G and 2I).

Efficient ZFN-Mediated Gene Targeting of the Endogenous *PIG-A* Gene in hESCs

Using the validated *PIG-A* ZFN pair L1/R2, we sought to develop a more efficient, precise, and generalizable method for gene targeting of the *PIG-A* gene without the need to use aerolysin selection. Compared with NHEJ, HR is a more precise method to

(B) One of the aerolysin-resistant colonies derived following expression of the L1 and R2 ZFN pairs was isolated and termed as GNAR. After expansion, GNAR cells display unique hESC morphology and markers such as TRA-1-60 and NANOG.
(C) GNAR cells exhibit a normal karyotype (46, XY).
(D) DNA sequence in *PIG-A* exon 6 in GNAR cells, compared with that from parental GGFP (H1) hESCs. A 7 bp deletion (blue) in the coding sequence was found, resulting in frameshift and a premature translational stop codon (red). The *PIG-A* ZFN target sites are underlined. A sequencing chromatogram of GNAR cells is shown below the sequence alignment, with an arrow indicating the deletion site.
(E) FACS analysis showing that GNAR cells have lost the expression of GPI-APs such as CD59. This defect can be rescued by the introduction of exogenous *PIG-A* cDNA (GNAR-PIGA). Dot plot was gated on GFP+ hESCs.
(F) GNAR cells show loss of GPI-APs such as alkaline phosphatase (APase) on the cell surface. Scale bar, 50 μm.
(G) BMP4-induced trophoblast lineage differentiation defect in GNAR cells indicated by loss of *hCG-α* expression. BMP4 treatment was carried out as described previously (Chen et al., 2008).
(H) Rate of teratoma formation of GNAR ESCs with or without PIG-A transgene expression. Zero out of nine injections showed teratoma formation monitored up to 4 months. These defects can be largely rescued by exogenous *PIG-A* cDNA expression.
(I) Differential sensitivities of GNAR and GNAR-PIG-A hESCs. GNAR cells lack complement inhibitory proteins such as CD59 and CD55, whereas PIG-A cDNA expression restored these GPI-APs on the cell surface. Under lower pH (pH = 6.4) that activates complement-mediated cell lysis, GNAR showed a significantly increased cell death monitored by Annexin V staining, compared with the GNAR-PIG-A cells or ESCs under normal pH (7.4, upper rows).

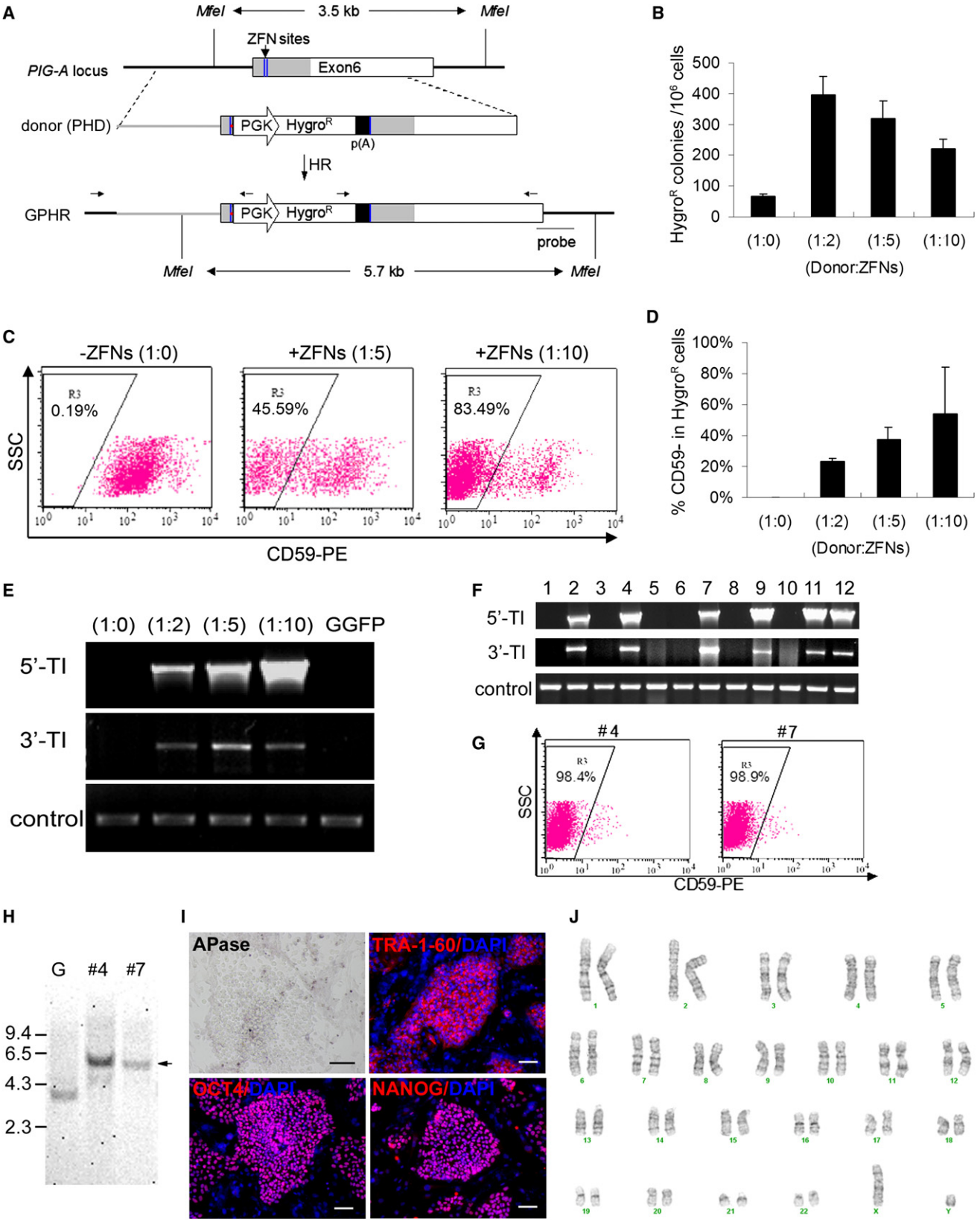
A
MfeI
3.5 kb
MfeI
ZFN sites
PIG-A locus
Exon6
donor (PHD)
PGK
Hygro^R
p(A)
HR
GPHR
PGK
Hygro^R
probe
MfeI
5.7 kb
MfeI
B
Hygro^R colonies /10^6 cells
500
400
300
200
100
0
(1:0)
(1:2)
(1:5)
(1:10)
(Donor:ZFNs)
C
-ZFNs (1:0)
+ZFNs (1:5)
+ZFNs (1:10)
R3
0.19%
R3
45.59%
R3
83.49%
SSC
CD59-PE
D
% CD59- in Hygro^R cells
100%
80%
60%
40%
20%
0%
(1:0)
(1:2)
(1:5)
(1:10)
(Donor:ZFNs)
E
(1:0) (1:2) (1:5) (1:10) GGFP
5'-TI
3'-TI
control
F
1 2 3 4 5 6 7 8 9 10 11 12
5'-TI
3'-TI
control
G
#4
#7
R3
98.4%
R3
98.9%
SSC
CD59-PE
H
G
#4
#7
9.4
6.5
4.3
2.3
I
APase
TRA-1-60/DAPI
OCT4/DAPI
NANOG/DAPI
J

mutate as well as correct a gene in a predetermined fashion. Thus, to inactivate the *PIG-A* gene by HR-mediated mutagenic insertion, we constructed a donor vector (called "PHD") in which a PGK-Hygro^R expression cassette was placed between two *PIG-A* homology arms (Figure 3A). Successful HR-mediated targeting will result in the insertion of the PGK-Hygro^R cassette into the coding region in exon 6 of the *PIG-A* gene, thereby inactivating the *PIG-A* gene (Figure 3A). By contrast, random insertion of PHD into transcriptionally active regions of the genome will also result in the formation of Hygro^R ES clones but will not disrupt the *PIG-A* gene. Thus, random insertions, unlike targeted insertions, will result in the continued cell-surface expression of GPI-APs.

We transfected the PHD-targeting plasmid into H1-derived GGFP hESCs in the presence or absence of vectors expressing the L1/R2 ZFN pair to target the endogenous *PIG-A* locus. Different ratios of donor versus ZFN expression vector DNA were tested (Figure 3B), and following transfection, cells were plated onto Hygro^R W3R feeder cells and selected for 12 days. ES-like colonies emerged under each transfection condition, and the number of colonies was quantified. In the absence of ZFNs, we obtained 67 ± 11 Hygro^R colonies per 10^6 input cells at transfection. The formation of Hygro^R colonies could be due to either random integration or HR. With ZFNs, however, we obtained significantly more Hygro^R colonies, ranging from 220 ± 54 to 395 ± 105 per 10^6 input cells (Figure 3B). After quantitation of Hygro^R ES colonies, all of the cells were analyzed for the presence or absence of GPI-APs such as CD59. When ZFNs were absent, background levels of CD59− cells were detected (0.19%), indicating that most, if not all, Hygro^R colonies resulted from random insertion of the PHD donor into loci other than *PIG-A*. In contrast, when ZFNs were present, CD59− cells were present at a high frequency of up to 83% (Figures 3C and 3D). To confirm the targeted insertion of PHD DNA into the *PIG-A* locus, we performed PCR analysis using a pair of specific primers that only amplify either the 5′ or 3′ junction of the predicted HR product (Figure 3E). Targeted insertion products were abundantly detected in Hygro^R cells obtained when ZFNs were used, but not in Hygro^R cells obtained when ZFNs were absent (Figure 3E).

To create knockout or knockin ESCs with a uniform genetic background, it is critical to isolate clonal cell lines following HR to ensure a homogenous population. With the improved HR efficiency we observed with ZFNs, we tested whether we could readily obtain *PIG-A* knockout clones (called "GPHR"). From 12 Hygro^R hESC colonies, 6 clones (50%) were confirmed to have undergone the predicted HR event at the *PIG-A* locus, as determined by PCR to detect the targeted insertion (Figure 3F) and by fluorescence-activated cell sorting (FACS) to detect the loss of GPI-APs (Figures 3G and S4A). Two out of six clones (#4 and #7) showed loss of CD59 in nearly all of the cells (Figure 3G), thereby validating their clonality. The clonality and the targeted insertion were further confirmed by Southern blot (Figure 3H). Furthermore, both of these clones showed normal karyotypes, undifferentiated hESC morphology, and expression of unique hESC markers (Figures 3I, 3J, and S5). As expected, the cell-surface expression of GPI-APs, such as APase, was absent in these GPHR clones (Figure 3I). The altered phenotypes of these GPHR clones, such as GPI-AP deficiency, could also be rescued by *PIG-A* transgene expression (Figure S4B), confirming that the GPI-AP deficiency in GPHR cells was solely due to *PIG-A* gene knockout.

Gene Targeting in the MP2 hiPSC Line with or without Using ZFNs

To our knowledge, there has been no published report to date describing gene targeting by any method in hiPSCs. Therefore, we investigated whether HR-mediated gene targeting could be achieved in hiPSCs using the PIG-A and EGFP* systems with or without the aid of ZFNs. The first of the two hiPSC lines that we used is MP2, which has previously been shown to be pluripotent (Mali et al., 2008). Using an optimized donor:ZFN ratio, we observed GFP+ colonies emerge 5 days following transfection of MP2 iPSCs harboring the mutated EGFP* template (Figure 4A). Gene correction efficiency reached 0.14% when the GFP-specific ZFN expression vectors were used in transfection, as compared to < 0.0001% when ZFN expression vectors were absent from the transfection (Figure 4B). These data demonstrate

Figure 3. Knockout of the Endogenous *PIG-A* Gene in hESCs by ZFN-Mediated Homologous Recombination

(A) Scheme of *PIG-A* gene knockout using ZFNs targeting the coding sequence (gray) within exon 6. The DNA sequences of the two half ZFN sites (blue lines) are shown in Figure S10. The HR donor (PHD) vector contains a PGK-Hygro^R-poly(A) expression cassette flanked by two arms of *PIG-A* homology sequences (2 kb left + 2 kb right). In the PHD vector, a frameshift mutation and stop codon (red dot) upstream of the PGK-Hygro^R-poly(A) cassette were introduced to replace the spacer sequence between the two ZFN sites. Two sets of PCR primers, indicated above the anticipated HR product (GPHR), were used to confirm the junctions of targeted insertion. A DNA probe further downstream of the *PIG-A* locus and outside of the right arm of PHD was used for Southern blot analysis.

(B) After nucleofection and drug selection, the number of Hygro^R colonies per million input cells was calculated and compared among different ratios of donor:ZFNs. The ratio (w/w) of 1:5 is equivalent to 1 donor for 4.2 DNA molecules of each ZFN. Six experiments were performed with the ratio of 1:5, and three experiments were performed for the remaining ratios.

(C) Representative FACS analysis of CD59, a GPI-AP, expressed in the Hygro^R cell population after gene targeting. Dot plot was gated on GFP+ hESCs.

(D) Summary of CD59− population in the Hygro^R cells from two experiments, as analyzed in (C).

(E) PCR analysis of genomic DNA confirms that targeted integration (TI) occurred in Hygro^R cells only when ZFNs were used and when GPI-AP-deficient cells were obtained. TI was detected by primer sets specific for 5′ and 3′ integration junctions as indicated in (A). An arbitrary genomic region (near *PIG-A* exon 4) was amplified as a positive DNA control.

(F) Twelve GPHR colonies were manually picked after Hygro^R selection following ZFN-mediated *PIG-A* knockout in GGFP cells. Six out of 12 showed targeted integration (TI).

(G) Two of the 12 colonies, 4 and 7, were shown to have nearly complete loss of CD59.

(H) Southern blot analysis of genomic DNA after *Mfe I* digestion confirmed that these two clones (4 and 7) contain expected targeted insertion at the *PIG-A* locus. Arrow indicates a longer *Mfe I* band (5.7 kb, due to the PGK-Hygro^R insertion) instead of a 3.5 kb band in parental GGFP (see Figure 3A). G, GGFP parental hESCs.

(I) Staining of one of the two clones, 4 (GPHRc4). This clone lacks APase, a GPI-AP, on the cell surface but maintains undifferentiated hESC markers such as TRA-1-60, OCT4, and NANOG. Scale bar, 50 μm. Similar data with clone 7 are shown in Figure S5.

(J) GPHRc4 (clone 4) cells exhibit a normal karyotype (46, XY). Similar data with clone 7 are shown in Figure S5.

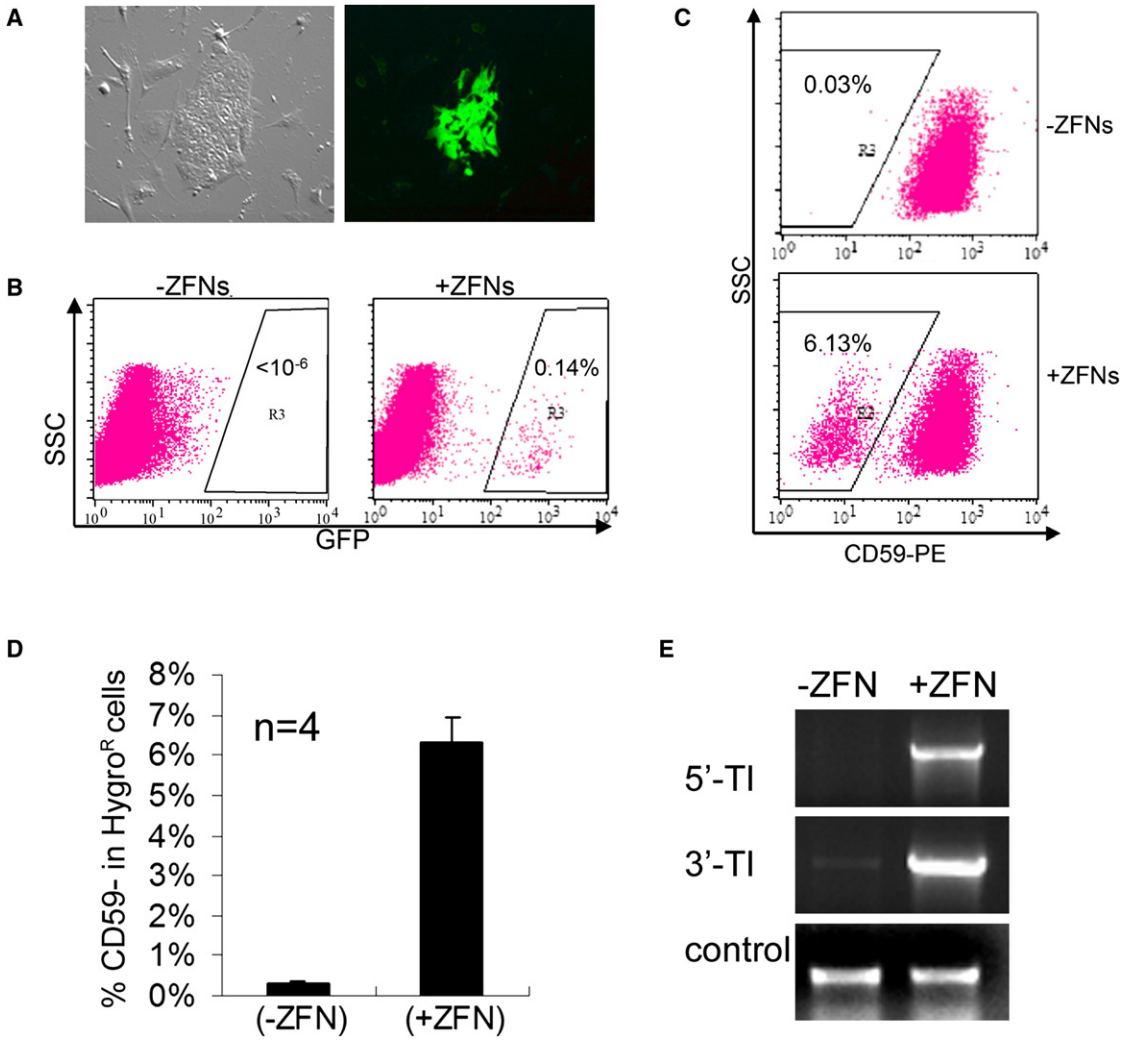

Figure 4. HR-Mediated Gene Targeting of EGFP and *PIG-A* Genes in Female Human MP2 iPSCs

(A) Microscopy of corrected (GFP+) MP2 iPSCs harboring the EGIP* reporter, 5 days after nucleofection with GFP-specific ZFNs.

(B) FACS analysis of EGFP gene correction in MP2 iPSCs with or without GFP-specific ZFNs. Dot plots were gated on TRA-1-60+ cells.

(C) *PIG-A* gene targeting in MP2 iPSCs with or without PIG-A-specific ZFNs was performed as described in Figure 3A using the 1:5 ratio of donor:ZFN DNA. After nucleofection and hygromycin B selection, TRA-1-60+ (hiPS/hES) cells were analyzed for the presence or absence of CD59 (a GPI-AP). Representative FACS dot plots are shown.

(D) Summary of FACS analysis of CD59− MP2 iPSC populations after *PIG-A* gene targeting from four independent experiments.

(E) PCR confirms the targeted integration into the *PIG-A* locus in MP2 iPSCs.

that the ZFNs stimulate gene correction by at least 1400-fold in human MP2 iPSCs. Because the mutated EGFP* target is not present in every one of starting MP2 cells (since they are already Puro^R and full selection of the EGIP* integration by puromycin resistance is not feasible), the number is likely an underestimate (Figures 4A and 4B).

Next, we carried out ZFN-mediated gene targeting at the endogenous *PIG-A* gene in MP2 hiPSCs (using the same strategy employed for ESCs; see Figure 3). We anticipated that the frequency with which we would obtain *PIG-A*-deficient MP2 cells would be lower than what we achieved in the hESCs because MP2 iPSCs are female (XX) in origin and thus contain two copies of the *PIG-A* gene. It is unclear currently whether the inactivated X chromosome inherited from the parental IMR90 fibroblasts remains inactivated or is activated in MP2 iPSCs after reprogramming. In the latter case, targeting both alleles of the *PIG-A* locus is required to generate a null phenotype. Following transfection of MP2 iPSCs with PHD donor DNA with or without *PIG-A*-specific ZFN expression vectors, we observed Hygro^R human ESC/iPSC-like colonies under both conditions. In four independent experiments, we found that, on average, 6.3 ± 0.7% of Hygro^R human cells are CD59− when the PIG-A ZFNs were used (Figures 4C and 4D), compared with background levels (<0.05%) when PIG-A ZFNs were not used. The targeted integration of the PGK-Hygro^R DNA cassette could also be easily detected in the ZFN-treated cells (Figure 4E).

HR-Mediated Gene Targeting of the Endogenous *PIG-A* Gene to Generate GPI-AP-Deficient iPSCs

To better analyze and quantify HR-mediated *PIG-A* gene targeting, we also performed experiments in a well-characterized male (XY) hiPSC line (Park et al., 2008). The hFib2-iPS5 cells were derived from dermal fibroblasts of an adult male and were shown previously to have a normal karyotype and full pluripotency (Park et al., 2008). Similar to hESCs in early passages, the newly established hFib2-iPS5 cells are delicate to expand and transfect. We optimized conditions for efficient transfection of these cells in the following ways. We initially followed the published method and passaged them as clumps after partial dissociation by collagenase digestion (Park et al., 2008). However, the method yielded poor transfection efficiencies using nucleofection or other transfection techniques (data not shown). We found that trypsin or accutase treatment generated smaller clumps and single cells that allowed us to achieve higher transient transfection efficiencies (Figure S6), but the survival rate was much lower. We found that treating with a ROCK inhibitor Y27632 before trypsin-mediated cell dissociation significantly improved the colony-forming efficiency of early passage hFib2-iPS5 (Figure S7), likely due to enhanced survival of single cells/small clumps as found for hESCs (Watanabe et al., 2007). The addition of Y27632 during and after nucleofection further helped the attachment/survival of single cells or smaller clumps (<30 cells) in culture after transfection. With these improvements, we transfected hFib2-iPS5 cells with the PHD HR donor with or without the *PIG-A* ZFN expression vectors, as we did for hESCs. Significantly more Hygro^R iPS colonies were obtained if Y27632 was present (Figure 5A). When the Hygro^R iPSCs were analyzed for the loss of GPI-APs such as CD59 (Figure 5B), up to 83% of the Hygro^R iPSCs were CD59− (average 45% ± 20%; Figure 5C) when ZFNs were used. In contrast, background levels (0.22% ± 0.04%) of CD59− cells were found when ZFNs were absent, even though these iPSCs were also Hygro^R (likely due to the PHD random integration). PCR analysis of harvested Hygro^R cells confirmed targeted integration of the PHD DNA into the genome of hFib2-iPS5 cells when ZFNs were present (Figure 5D). Without ZFNs, the resulting Hygro^R iPSCs were neither CD59− nor showing the targeted integration (Figure 5D), suggesting that they indeed resulted from random integration of the PHD donor. Therefore, the *PIG-A*-specific ZFNs confer a > 200-fold increase in the efficiency of *PIG-A* gene targeting, equivalent to that observed in hESCs (Figure 3D).

To molecularly characterize the targeting events, we randomly picked nine Hygro^R iPSC colonies from treated cells after cotransfection of PHD and ZFN-expression plasmids. We successfully expanded cells from eight colonies and analyzed them by PCR to detect the targeted insertion (Figure 5E), by Southern blot to confirm HR at the *PIG-A* locus (Figure 5F), and by FACS analysis to confirm the loss of GPI-APs due to a *PIG-A* null mutation (Figure S6). Five out of the eight hFib2-iPS5 *PIG-A* HR (FPHR) colonies (62.5%) that we analyzed had the targeted insertion at the *PIG-A* locus (Figures 5E and 5F). Three of them (colonies c1, c6, and c8) contained only the targeted *PIG-A* allele and homogenously lacked GPI-AP expression (Figures 5F and S6), suggesting a clonal origin for each picked colony. We found that the donor DNA is present only in the targeted locus in these three homogenous FPHR clones (Figure S8A). By a more sensitive PCR-mediated method, we did not detect the presence of the ZFN DNA in the genome of the three clones (Figure S8B). The homogenous iPSCs such as clone FPHR c1 lost the expression of GPI-APs but retained undifferentiated iPSC/ESC morphology and the expression of pluripotency markers (Figure 5G). The differentiation potential of FPHRc1 iPSCs was similar to the *PIG-A* null human ESCs based on the in vitro assays described in Figure 2 (data not shown). Two randomly selected iPS clones (c1 and c6) retained a normal karyotype after HR-mediated gene targeting and expansion (Figure 5H). In summary, successful correction of the mutated EGFP gene and mutation of the endogenous *PIG-A* gene by HR show that ZFNs can stimulate gene targeting in hiPSCs by at least several hundred-fold. This degree of stimulation is sufficient to enable the isolation of clonal populations of iPSCs with the desired genetic modification.

DISCUSSION

The importance of making a specific genetic modification in hPSCs has been widely recognized (Giudice and Trounson, 2008). The creation or correction of a specific mutation by HR-mediated gene targeting ensures permanent genetic alterations, a capability that will be of great utility in stem cell research and for potential applications of hPSCs in therapeutic uses. In 2003 and 2004, two landmark papers demonstrated the feasibility of gene targeting by HR in hESCs (Urbach et al., 2004; Zwaka and Thomson, 2003). Four more papers (Costa et al., 2007; Davis et al., 2008; Di Domenico et al., 2008; Irion et al., 2007) in the past 2 years confirmed HR-mediated gene targeting in hESCs using a plasmid-based delivery method. These studies collectively demonstrated that HR is feasible in hESCs but is technically challenging because of the low rate (<10^{-6}) using standard targeting strategies. These technical limitations have limited the broad use of targeting in hPSCs, and a general approach that increases the efficiency of targeting would increase the range of experimental and potentially therapeutic uses of these cells.

One strategy to increase the rate of gene targeting in hPSCs is to use highly specific ZFNs. ZFN-induced DSBs at specific sequences have been used to stimulate targeting efficiencies in a wide range of cell types and organisms (Carroll, 2008; Cathomen and Joung, 2008) and were recently shown to stimulate gene targeting in two hESC lines (Lombardo et al., 2007). The strength and weakness of this pioneering paper that used ZFNs (efficiently delivered by IDLV vectors) to achieve gene targeting in multiple cell types, including hESCs, have been discussed comprehensively (Giudice and Trounson, 2008). Another limitation of this study is that the two hESC lines used, HUES1 and HUES3, are prone to have karyotypic abnormalities after prolonged culture (Cowan et al., 2004). Moreover, an analysis of whether ZFNs might induce unwanted chromosomal rearrangements and changes in growth parameters was absent (Lombardo et al., 2007). In the present study, we have demonstrated that (1) ZFNs can be used to stimulate gene targeting in hPSCs, including iPSCs, without inducing karyotypic changes or changes in their pluripotent potential, (2) defined phenotypic changes can be rationally created by the use of ZFN-mediated gene targeting, (3) clonal cell lines with targeted genetic modifications can be derived and expanded, and (4) nonviral methods

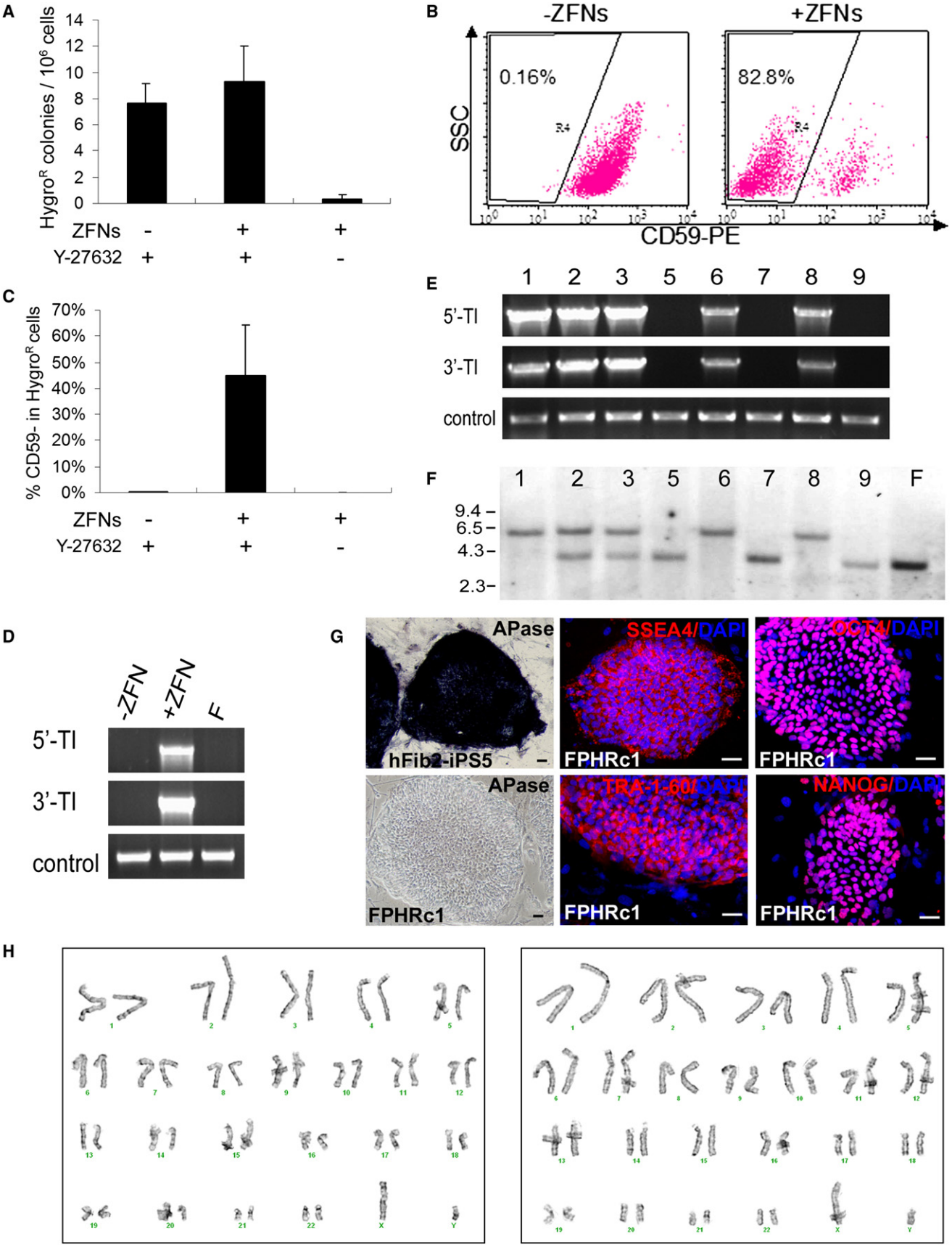
A
Hygro^R colonies / 10^6 cells
14
12
10
8
6
4
2
0
ZFNs - + +
Y-27632 + + -
B
-ZFNs
+ZFNs
0.16%
82.8%
R4
SSC
CD59-PE
C
% CD59- in Hygro^R cells
70%
60%
50%
40%
30%
20%
10%
0%
ZFNs - + +
Y-27632 + + -
D
-ZFN
+ZFN
F
5'-TI
3'-TI
control
E
1 2 3 5 6 7 8 9
5'-TI
3'-TI
control
F
1 2 3 5 6 7 8 9 F
9.4
6.5
4.3
2.3
G
APase
hFib2-iPS5
FPHRc1
SSEA4/DAPI
OCT4/DAPI
TRA-1-60/DAPI
NANOG/DAPI
H

of inducing gene targeting using ZFNs can be used in hPSCs. These results are discussed in more detail below.

We used a virus-free DNA delivery system and successfully targeted two different genes in karyotypically normal hESCs and hiPSCs. Our studies were performed using novel ZFNs targeting a disease-related gene (*PIG-A*) as well as the previously described ZFNs targeting the EGFP gene (Pruett-Miller et al., 2008). Using optimized ratios of donor DNA and ZFN-expressing plasmid vectors, as well as an improved method of DNA delivery, our protocol allowed us to achieve high efficiencies (stimulations of 200- to 2000-fold more than the rate without ZFNs) of HR-mediated gene targeting in either creating a mutation in the endogenous *PIG-A* gene or correcting a chromosomally integrated mutant EGFP gene in both hESCs and iPSCs. Despite using homology arms (a total of 2 kb) that would be considered too short using standard targeting strategies (Di Domenico et al., 2008; Suzuki et al., 2008), we achieved a gene correction rate of 0.14%–0.24% in hESCs and hiPSCs cotransfected with a pair of GFP-targeted ZFNs (Figures 1 and 4). Similarly, the gene-targeting efficiency at the endogenous *PIG-A* gene was also high when a pair of ZFNs was used together with a donor vector containing short (and thus suboptimal) homology arms (a total of 4 kb). This approach should be applicable to any gene of interest for which a pair of highly active and specific ZFNs is generated and to other methods for more efficient DNA delivery (Lombardo et al., 2007; Suzuki et al., 2008).

We found that both hESCs and hiPSCs that had been targeted using ZFNs had no karyotypic abnormalities and did not exhibit any alteration in their pluripotent properties, even after extended expansion to accumulate sufficient cells required for comprehensive cellular and molecular analyses. In addition, phenotypic and biological defects of PIG-A null hESCs GNAR (created by ZFN-mediated NHEJ) and GPHR (created by ZFN-mediated HR) could be rescued by expression of a *PIG-A* transgene. Together, these data suggest that undesired genome alterations by a pair of high-quality and validated ZFNs are minimal. However, we note that acute ZFN-mediated cell toxicity could be observed when ZFNs were used at a higher concentration with the nucleofection (Figure 3B) or the Lipofectamine 2000 transfection methods (data not shown). Long-term and off-target effects of ZFNs remain to be fully characterized. Although major alteration of genome due to off-target DSBs usually results in cell death and elimination of affected cells, minor changes such as small deletions and additions could be carried on in the surviving population. It has been difficult to locate in the whole genome a small alteration induced by off-target DSBs. It is now possible to detect such abnormality by comparing parental and targeted cell lines using advanced technologies such as genome-wide, high-resolution SNP analysis and ideally whole-genome (deep) DNA sequencing. In addition to using ZFNs that possess high-quality zinc finger DNA-binding domains (as was done in this report), two other strategies to reduce off-target effects of ZFNs have been described. The first one uses modifications of the nuclease domain to minimize homodimerization of ZFNs, which may lead to cleavage at off-target sites (Miller et al., 2007; Pruett-Miller et al., 2008; Szczepek et al., 2007). The second one uses small molecules to attenuate the extent and timing of ZFN expression (Pruett-Miller et al., 2009). It will be interesting to determine the degree to which these strategies minimize the off-target effects and toxicity of ZFNs when they are utilized with ZFNs in hPSCs. The ability to expand a few desirable ES or iPS clones unlimitedly alleviates the need to achieve perfection in every single cell using ZFN-mediated HR. Gene targeting at the level of hiPSCs and hESCs with unlimited self-renewal capacity also allows for the full characterization of genomic integrity before the use of the selected iPS and ES clones that have undergone gene-targeting events. Taken together, the studies reported here demonstrate that high-quality ZFNs made by using the recently described OPEN platform can induce highly efficient gene targeting in hESCs and iPSCs with minimal toxicity and karyotypic alterations. The OPEN method was developed by the Zinc Finger Consortium (http://www.zincfingers.org) and accounts for context-dependent DNA-binding activities of zinc fingers. OPEN ZFNs have been previously used to modify three human genes (Maeder et al., 2008), five zebrafish genes (Foley et al., 2009), and plant genes (Maeder et al., 2008; Townsend et al., 2009). The results of this report extend the number of endogenous human genes modified by OPEN ZFNs and demonstrate that OPEN ZFNs can be used in more than just somatic human cells. Importantly, the reagents and protocols that are needed to make ZFNs by the OPEN method are publicly available, and therefore, any interested academic laboratory can use the approach to engineer

Figure 5. HR-Mediated *PIG-A* Gene Targeting in Male hiPSCs, Generating Clonal *PIG-A* Null iPSCs

(A) *PIG-A* knockout was performed in hFib2-iPS5 cells derived from adult (male) fibroblasts, using the strategy shown in Figure 3A. A nucleofection protocol similar to that used for hESCs was carried out, except ROCK inhibitor (Y27632) was added. Mean and SEM of Hygro^R colonies per million of input cells from three independent experiments are presented.

(B) FACS analysis of *PIG-A* knockout in hFib2-iPS5 cells with or without ZFNs in the presence of ROCK inhibitor Y27632. TRA-1-60+ (hiPS) cells were gated and analyzed for the presence or absence of CD59. Representative dot plots are shown here.

(C) Comparisons of percentages of CD59− cells in Hygro^R hFib2-iPS5 cells after *PIG-A* gene targeting using various treatments, as described above. n = 3.

(D) PCR analysis confirms that Hygro^R hFib2-iPS5 cells contain targeted integration after ZFN-mediated HR treatment. F, parental hFib2-iPS5 cells.

(E) PCR analysis shows targeted integration in five out of eight hFib2-iPS5 colonies that we expanded and examined.

(F) Southern blot analysis detects the presence of the targeted (5.7 kb) and the wild-type (3.5 kb) *PIG-A* alleles (see a diagram in Figure 3A). The expected HR product (the targeted insertion) is found in the same five colonies that are positive by PCR detection (E). Three of them (c1, c6, and c8) appear to be homogeneous *PIG-A* knockout hFib2-iPS5 clones (FPHR) showing only the targeted allele (5.7 kb). Two (c2 and c3) contain both the targeted and the wild-type alleles. Because the hFib2-iPS5 cells (male, XY) have only one *PIG-A* allele in the X chromosome, this is likely due to the fact that the colony picked after hygromycin selection is not from a single clone and, instead, is from mixed cells. The remaining three Hygro^R colonies result from off-target insertion, showing only the wild-type *PIG-A* allele as the parental hFib2-iPS5 cells (F). The Southern blot data are highly consistent with the pattern of GPI-AP expression in the eight analyzed colonies (Figure S6B).

(G) Staining of the FPHRc1 (PIG-A knockout) iPS clone shows loss of APase (a GPI-AP) on the cell surface, compared to the parental hFib2-iPS5 cells, but maintains the expression of pluripotency markers (TRA-1-60, SSEA-4, OCT4, and NANOG). Scale bar, 50 μm.

(H) FPHRc1 (left) and FPHRc6 (right) clones retain a normal karyotype (46, XY).

customized ZFNs for their target gene of interest in a variety of cell types such as hPSCs.

Our report provides the first demonstration of hiPSCs modified by HR and demonstrates the feasibility and efficiency of an approach that can be used for creating or correcting specific mutations. Using the endogenous *PIG-A* gene and a chromosomally integrated GFP gene as targets, we demonstrated that our improved protocol of delivering gene-targeting donor and ZFN-expressing plasmids works efficiently for hiPSCs as well as hESCs. A major difference that we observed is that early passage iPSCs, especially those passaged by collagenase as cell clumps, survive poorly if they are harvested by trypsin as smaller cell clumps or single cells required by the nucleofection method. However, treating hiPSCs by adding a ROCK inhibitor Y27632 before trypsin-mediated cell dissociation and during the nucleofection significantly improved the survival of transfected hiPSCs and the formation of $Hygro^R$ colonies (Figure 5A). The overall HR efficiency measured by the *PIG-A* gene targeting in the newly established hiPSC lines is still lower than that in the well-adapted hESC lines such as the H1/GGFP line. This is due, at least in part, to the poor colony-forming efficiency of hFib2-iPS5 cells, which is > 8- to 9-fold lower than that of H1/GGFP hESCs (Figure S7). Despite all of the current limitations in cell culture, resulting in a lower number of total $Hygro^R$ colonies per million of input hFib2-iPS5 cells, we are still able to generate a cell population containing > 40% PIG-A-deficient cells after drug selection and to isolate true PIG-A knockout iPS clones from this XY iPSC line. Together with the data using a different hiPS line (MP2), we showed for the first time that an endogenous gene can be efficiently targeted in hiPSCs, demonstrating the potential of using gene targeting in research and clinical applications of disease-specific hiPSCs. Possible future uses of gene targeting in hiPSCs include (1) increasing the efficiency of creating conditional alleles using the Cre-Lox system (Irion et al., 2007), (2) correcting disease-causing mutations in X-linked or autosomal genetic diseases, (3) using gene targeting to create better models of human disease in hiPSCs, (4) using serial gene targeting by HR to create precise biallelic modifications in autosomal genes or X-linked genes in female cells, and (5) using HR to correct disease-causing mutations in patient-specific iPSCs and using the genetically corrected cells to cure a disease, as recently demonstrated in a mouse model (Hanna et al., 2007).

Previous studies have demonstrated that even genes that are not transcriptionally active in undifferentiated hESCs, such as *MIXL1*, *CCR5*, and *FEZF2*, can be successfully targeted (Davis et al., 2008; Lombardo et al., 2007; Ruby and Zheng, 2009), as has been observed in numerous cases of mouse ESC studies. Enhancement of ZFNs on gene targeting of *CCR5* has been previously demonstrated in the two hESC lines used (Lombardo et al., 2007). Thus, with the aid of ZFNs that greatly enhance the HR efficiency in hESCs and hiPSCs, we are optimistic that we will also be able to achieve gene targeting in iPSCs that are not expressed in the undifferentiated state. The experimental systems that we described here, i.e., the validated HR donor constructs and ZFNs for two genes (EGFP and *PIG-A*) with simply phenotypic readouts, will further help investigators to optimize gene targeting in hiPSCs and hESCs with or without a pair of ZFNs. Thus, our present study provides a solid foundation for researchers interested in the efficient correcting or mutating of a specific endogenous gene in both hiPSCs and hESCs.

EXPERIMENTAL PROCEDURES

Culture of hESCs and hiPSCs

Human H1 and H9 ESC lines were obtained from WiCell Research Institute and cultured as previously described (Chen et al., 2008; Yu et al., 2008). GGFP derived from H1 ESCs with stable GFP expression by the lentiviral transduction (Dravid et al., 2005) was used in *PIG-A* gene targeting. MP2 iPS and hFib2-iPS5 cells were passaged by collagenase and cultured as previously described (Mali et al., 2008; Park et al., 2008).

Engineering of PIG-A-Specific ZFNs

ZFNs specific for a target site within the PIG-A coding sequence (Figure S10) were engineered using the OPEN method as previously described (Maeder et al., 2008). The top two of three zinc finger arrays for each half-site that exhibited the highest levels of transcriptional activation in the bacterial two-hybrid system were chosen for use as ZFNs. To construct ZFN expression vectors for mammalian cells, XbaI-BamHI fragments harboring the engineered zinc finger arrays were cloned into XbaI- and BamHI-digested pST1374 and fused to the endonuclease domain in the vector (Maeder et al., 2008). A pair of ZFNs targeting the GFP gene was previously described (Pruett-Miller et al., 2008). The target site and amino acid sequences of these two GFP-specific ZFNs are also shown in Figure S9. They are expressed from a similar expression vector. Requests for OPEN ZFN reagents and protocols should be directed to JKJ.

EGFP Gene Correction in 293T Cells

First, EGFP was mutated with either a 35 bp insertion (Figure S2) or a 41 bp insertion containing *PIG-A* ZFN sites (Figure S3) and inserted into a lentiviral vector with IRES-$Puro^R$ cassette (Figure 1A). After transduction and puromycin selection, surviving cells containing EGIP* (termed 293T-EGIP* or 293T-EGIP* PIGA) were used for EGFP gene targeting. The 2.5×10^5 293T-EGIP* or 293T-EGIP*PIGA cells were plated in one 12-well coated with 0.1% gelatin 1 day before lipofection. At the day of transfection, 1 μg of tGFP donor with various amounts of ZFNs expression vectors was transfected using standard Lipofectamine 2000 protocol (Invitrogen). GFP+ cells started to show up at 2.5 days after transfection and were monitored by FACS and microscopy thereafter.

EGFP Gene Correction in hESCs and hiPSCs

H9 hESCs were transduced with EGIP* (35 bp insertion) lentivirus and selected with puromycin (1 μg/ml), and therefore, the starting population harbors EGIP* template. The 5×10^6 H9-EGIP* cells grown on MEF feeder cells were harvested at ~80% confluence with brief trypsin digestion and pipetting. Then, the cells were resuspended in 100 μl Amaxa mouse ES nucleofection buffer with various ratios of tGFP donor:ZFNs (e.g., 1:10 = 1 μg:10 μg) and transfected using the Nucleofector II and preset programs such as A-23 (Amaxa). Cells were replated 1:1 onto MEFs afterward, and GFP+ cells began to emerge 4–5 days later. For MP2 iPSCs that are already puromycin resistant, no puromycin selection was done, and therefore, only a portion of the starting population has the EGIP* template. The 3×10^6 mixed MP2-EGIP* cells (without puromycin-mediated transgene selection) were used for EGFP gene correction with the same nucleofection settings as for H9-EGIP* cells.

PIG-A Gene Targeting in hESCs and iPSCs

GGFP hESCs, MP2 iPSCs, or hFib2-iPS5 cells ($3–5 \times 10^6$) were transfected with 4 μg of *PIG-A*-targeting donor (PHD) and various amounts of the L1/R2 ZFN pair (Figure S10). Transfected cells were then replated onto W3R feeders (Cai et al., 2007) and selected with conditioned medium containing hygromycin (10 μg/ml) for 12 days beginning from day 4 postnucleofection. In hFib2-iPS5 cell gene-targeting experiments, 10 μM ROCK inhibitor Y27632 (Watanabe et al., 2007) was added for 1 hr prior to and 24 hr postnucleofection. Hygromycin-resistant colonies were counted after selection, and single colonies were manually picked and expanded.

More details are provided in the Supplemental Data.

SUPPLEMENTAL DATA

Supplemental Data include Supplemental Experimental Procedures and 10 figures and can be found with this article online at http://www.cell.com/cell-stem-cell/supplemental/S1934-5909(09)00232-X.

ACKNOWLEDGMENTS

We thank Sarah Dowey and the Johns Hopkins Hospital Prenatal Cytogenetics Laboratory for professional karyotyping. We also thank three anonymous reviewers for suggestions that helped us in revision. This work is funded in part by the Stem Cell Research Foundation (S2005-026), Johns Hopkins Institute for Cell Engineering, and the NIH grant R01 HL073781 to L.C. J.Z. is supported by a Maryland Stem Cell Research Postdoctoral Fellowship Grant. J.K.J.'s group is supported by the NIH (R01GM069906, R21RR024189, and R21HL091808), the Cystic Fibrosis Foundation, and the MGH Pathology Service. M.H.P.'s lab is supported by the state of Texas, NIH RO1 HL079295, and by a Career Development Award from the Burroughs-Wellcome Fund. G.Q.D. is an Investigator of Howard Hughes Medical Institute.

Received: February 25, 2009
Revised: April 24, 2009
Accepted: May 20, 2009
Published online: June 18, 2009

REFERENCES

Cai, L., Ye, Z., Zhou, B.Y., Mali, P., Zhou, C., and Cheng, L. (2007). Promoting human embryonic stem cell renewal or differentiation by modulating Wnt signal and culture conditions. Cell Res. *17*, 62–72.

Carroll, D. (2008). Progress and prospects: Zinc-finger nucleases as gene therapy agents. Gene Ther. *15*, 1463–1468.

Cathomen, T., and Joung, J.K. (2008). Zinc-finger nucleases: the next generation emerges. Mol. Ther. *16*, 1200–1207.

Chen, G., Ye, Z., Yu, X., Zou, J., Mali, P., Brodsky, R.A., and Cheng, L. (2008). Trophoblast differentiation defect in human embryonic stem cells lacking PIG-A and GPI-anchored cell-surface proteins. Cell Stem Cell *2*, 345–355.

Costa, M., Dottori, M., Sourris, K., Jamshidi, P., Hatzistavrou, T., Davis, R., Azzola, L., Jackson, S., Lim, S.M., Pera, M., et al. (2007). A method for genetic modification of human embryonic stem cells using electroporation. Nat. Protoc. *2*, 792–796.

Cowan, C.A., Klimanskaya, I., McMahon, J., Atienza, J., Witmyer, J., Zucker, J.P., Wang, S., Morton, C.C., McMahon, A.P., Powers, D., et al. (2004). Derivation of embryonic stem-cell lines from human blastocysts. N. Engl. J. Med. *350*, 1353–1356.

Davis, R.P., Ng, E.S., Costa, M., Mossman, A.K., Sourris, K., Elefanty, A.G., and Stanley, E.G. (2008). Targeting a GFP reporter gene to the MIXL1 locus of human embryonic stem cells identifies human primitive streak-like cells and enables isolation of primitive hematopoietic precursors. Blood *111*, 1876–1884.

Di Domenico, A.I., Christodoulou, I., Pells, S.C., McWhir, J., and Thomson, A.J. (2008). Sequential genetic modification of the hprt locus in human ESCs combining gene targeting and recombinase-mediated cassette exchange. Cloning Stem Cells *10*, 217–230.

Dravid, G., Ye, Z., Hammond, H., Chen, G., Pyle, A., Donovan, P., Yu, X., and Cheng, L. (2005). Defining the role of Wnt/beta-catenin signaling in the survival, proliferation, and self-renewal of human embryonic stem cells. Stem Cells *23*, 1489–1501.

Durai, S., Mani, M., Kandavelou, K., Wu, J., Porteus, M.H., and Chandrasegaran, S. (2005). Zinc finger nucleases: custom-designed molecular scissors for genome engineering of plant and mammalian cells. Nucleic Acids Res. *33*, 5978–5990.

Foley, J.E., Yeh, J.R., Maeder, M.L., Reyon, D., Sander, J.D., Peterson, R.T., and Joung, J.K. (2009). Rapid mutation of endogenous zebrafish genes using zinc finger nucleases made by Oligomerized Pool ENgineering (OPEN). PLoS ONE *4*, e4348.

Giudice, A., and Trounson, A. (2008). Genetic modification of human embryonic stem cells for derivation of target cells. Cell Stem Cell *2*, 422–433.

Hanna, J., Wernig, M., Markoulaki, S., Sun, C.W., Meissner, A., Cassady, J.P., Beard, C., Brambrink, T., Wu, L.C., Townes, T.M., et al. (2007). Treatment of sickle cell anemia mouse model with iPS cells generated from autologous skin. Science *318*, 1920–1923.

Hohenstein, K.A., Pyle, A.D., Chern, J.Y., Lock, L.F., and Donovan, P.J. (2008). Nucleofection mediates high-efficiency stable gene knockdown and transgene expression in human embryonic stem cells. Stem Cells *26*, 1436–1443.

Irion, S., Luche, H., Gadue, P., Fehling, H.J., Kennedy, M., and Keller, G. (2007). Identification and targeting of the ROSA26 locus in human embryonic stem cells. Nat. Biotechnol. *25*, 1477–1482.

Lombardo, A., Genovese, P., Beausejour, C.M., Colleoni, S., Lee, Y.L., Kim, K.A., Ando, D., Urnov, F.D., Galli, C., Gregory, P.D., et al. (2007). Gene editing in human stem cells using zinc finger nucleases and integrase-defective lentiviral vector delivery. Nat. Biotechnol. *25*, 1298–1306.

Lowry, W.E., Richter, L., Yachechko, R., Pyle, A.D., Tchieu, J., Sridharan, R., Clark, A.T., and Plath, K. (2008). Generation of human induced pluripotent stem cells from dermal fibroblasts. Proc. Natl. Acad. Sci. USA *105*, 2883–2888.

Maeder, M.L., Thibodeau-Beganny, S., Osiak, A., Wright, D.A., Anthony, R.M., Eichtinger, M., Jiang, T., Foley, J.E., Winfrey, R.J., Townsend, J.A., et al. (2008). Rapid "open-source" engineering of customized zinc-finger nucleases for highly efficient gene modification. Mol. Cell *31*, 294–301.

Mali, P., Ye, Z., Hammond, H.H., Yu, X., Lin, J., Chen, G., Zou, J., and Cheng, L. (2008). Improved efficiency and pace of generating induced pluripotent stem cells from human adult and fetal fibroblasts. Stem Cells *26*, 1998–2005.

Miller, J.C., Holmes, M.C., Wang, J., Guschin, D.Y., Lee, Y.L., Rupniewski, I., Beausejour, C.M., Waite, A.J., Wang, N.S., Kim, K.A., et al. (2007). An improved zinc-finger nuclease architecture for highly specific genome editing. Nat. Biotechnol. *25*, 778–785.

Nightingale, S.J., Hollis, R.P., Pepper, K.A., Petersen, D., Yu, X.J., Yang, C., Bahner, I., and Kohn, D.B. (2006). Transient gene expression by nonintegrating lentiviral vectors. Mol. Ther. *13*, 1121–1132.

Park, I.H., Zhao, R., West, J.A., Yabuuchi, A., Huo, H., Ince, T.A., Lerou, P.H., Lensch, M.W., and Daley, G.Q. (2008). Reprogramming of human somatic cells to pluripotency with defined factors. Nature *451*, 141–146.

Porteus, M.H. (2006). Mammalian gene targeting with designed zinc finger nucleases. Mol. Ther. *13*, 438–446.

Porteus, M.H., and Baltimore, D. (2003). Chimeric nucleases stimulate gene targeting in human cells. Science *300*, 763.

Porteus, M.H., and Carroll, D. (2005). Gene targeting using zinc finger nucleases. Nat. Biotechnol. *23*, 967–973.

Pruett-Miller, S.M., Connelly, J.P., Maeder, M.L., Joung, J.K., and Porteus, M.H. (2008). Comparison of zinc finger nucleases for use in gene targeting in mammalian cells. Mol. Ther. *16*, 707–717.

Pruett-Miller, S.M., Reading, D.W., Porter, S.N., and Porteus, M.H. (2009). Attenuation of zinc finger nuclease toxicity by small-molecule regulation of protein levels. PLoS Genet. *5*, e1000376.

Reubinoff, B.E., Pera, M.F., Fong, C.Y., Trounson, A., and Bongso, A. (2000). Embryonic stem cell lines from human blastocysts: somatic differentiation in vitro. Nat. Biotechnol. *18*, 399–404.

Ruby, K.M., and Zheng, B. (2009). Gene targeting in an HUES line of human embryonic stem cells via electroporation. Stem Cells, in press. Published online March 29, 2009. 10.1002/stem.73.

Suzuki, K., Mitsui, K., Aizawa, E., Hasegawa, K., Kawase, E., Yamagishi, T., Shimizu, Y., Suemori, H., Nakatsuji, N., and Mitani, K. (2008). Highly efficient transient gene expression and gene targeting in primate embryonic stem cells with helper-dependent adenoviral vectors. Proc. Natl. Acad. Sci. USA *105*, 13781–13786.

Szczepek, M., Brondani, V., Buchel, J., Serrano, L., Segal, D.J., and Cathomen, T. (2007). Structure-based redesign of the dimerization interface reduces the toxicity of zinc-finger nucleases. Nat. Biotechnol. *25*, 786–793.

Takahashi, K., Tanabe, K., Ohnuki, M., Narita, M., Ichisaka, T., Tomoda, K., and Yamanaka, S. (2007). Induction of pluripotent stem cells from adult human fibroblasts by defined factors. Cell *131*, 861–872.

Thomson, J.A., Itskovitz-Eldor, J., Shapiro, S.S., Waknitz, M.A., Swiergiel, J.J., Marshall, V.S., and Jones, J.M. (1998). Embryonic stem cell lines derived from human blastocysts. Science *282*, 1145–1147.

Townsend, J.A., Wright, D.A., Winfrey, R.J., Fu, F., Maeder, M.L., Joung, J.K., and Voytas, D.F. (2009). High-frequency modification of plant genes using engineered zinc finger nucleases. Nature *459*, 442–445.

Urbach, A., Schuldiner, M., and Benvenisty, N. (2004). Modeling for Lesch-Nyhan disease by gene targeting in human embryonic stem cells. Stem Cells *22*, 635–641.

Urnov, F.D., Miller, J.C., Lee, Y.L., Beausejour, C.M., Rock, J.M., Augustus, S., Jamieson, A.C., Porteus, M.H., Gregory, P.D., and Holmes, M.C. (2005). Highly efficient endogenous human gene correction using designed zinc-finger nucleases. Nature *435*, 646–651.

Watanabe, K., Ueno, M., Kamiya, D., Nishiyama, A., Matsumura, M., Wataya, T., Takahashi, J.B., Nishikawa, S., Muguruma, K., and Sasai, Y. (2007). A ROCK inhibitor permits survival of dissociated human embryonic stem cells. Nat. Biotechnol. *25*, 681–686.

Yang, T.T., Cheng, L., and Kain, S.R. (1996). Optimized codon usage and chromophore mutations provide enhanced sensitivity with the green fluorescent protein. Nucleic Acids Res. *24*, 4592–4593.

Yu, J., Vodyanik, M.A., Smuga-Otto, K., Antosiewicz-Bourget, J., Frane, J.L., Tian, S., Nie, J., Jonsdottir, G.A., Ruotti, V., Stewart, R., et al. (2007). Induced pluripotent stem cell lines derived from human somatic cells. Science *318*, 1917–1920.

Yu, X., Zou, J., Ye, Z., Hammond, H., Chen, G., Tokunaga, A., Mali, P., Li, Y.M., Civin, C., Gaiano, N., et al. (2008). Notch signaling activation in human embryonic stem cells is required for embryonic, but not trophoblastic, lineage commitment. Cell Stem Cell *2*, 461–471.

Zwaka, T.P., and Thomson, J.A. (2003). Homologous recombination in human embryonic stem cells. Nat. Biotechnol. *21*, 319–321.